

Radiative Pionic Decays of  $\Sigma^\pm$  Hyperons\*

ROBERT D. YOUNG,† MASAO SUGAWARA, AND TETSURO SAKUMA‡

*Department of Physics, Purdue University, Lafayette, Indiana*

(Received 25 October 1965)

The radiative decays  $\Sigma^\pm \rightarrow n + \pi^\pm + \gamma$  are analyzed on the assumption that the pole approximation is valid for the decays  $\Sigma^\pm \rightarrow n + \pi^\pm$ . It is shown that the matrix elements for these radiative decays are essentially the same as those for the phenomenological inner-bremsstrahlung diagrams as long as the anomalous magnetic moments of the  $\Sigma$  and  $\Lambda$  hyperons are at most of the order of magnitude of the nucleon magnetic moments. This is true independently of the signs and magnitudes of the strong and weak vertices involved. The branching ratios of  $\Sigma^\pm \rightarrow n + \pi^\pm + \gamma$  to  $\Sigma^\pm \rightarrow n + \pi^\pm$  depend on whether the pion in  $\Sigma^\pm \rightarrow n + \pi^\pm$  is in the  $S$ - or the  $P$ -wave state, in general agreement with what was pointed out by previous authors. However, in contrast with the results of the previous calculation, the present analysis shows that the anomalous magnetic moments of  $\Sigma^\pm$  and the neutron noticeably contribute to the branching ratios. Therefore, in order to check the underlying theoretical assumptions so as to determine the pion-wave assignment in  $\Sigma^\pm \rightarrow n + \pi^\pm$ , it is necessary to have either very accurate data for  $\Sigma^\pm \rightarrow n + \pi^\pm + \gamma$  or an experimental determination of the anomalous magnetic moments of  $\Sigma^\pm$ .

## I. INTRODUCTION

THE small asymmetry parameters in the decays  $\Sigma^\pm \rightarrow n + \pi^\pm$  show that the pions in these decays are in essentially pure angular-momentum states.<sup>1</sup> This fact, combined with the  $\Delta I = \frac{1}{2}$  rule, requires that the pions are in different angular-momentum states.<sup>2</sup> These are either the  $S$ - or the  $P$ -wave states according to the conservation of angular momentum. The experimental determination of this pion-wave assignment is of considerable importance since any successful theory of the weak interaction must be consistent with the correct assignment.

The most direct way to determine the pion-wave assignment is to measure the neutron polarization in the pionic decays of polarized  $\Sigma^\pm$  hyperons.<sup>3</sup> Since the neutron-polarization experiment is still very difficult to perform, Barshay, Nauenberg, and Schultz<sup>4</sup> have proposed that the radiative pionic decays  $\Sigma^\pm \rightarrow n + \pi^\pm + \gamma$  can be used to determine the pion-wave assignment in  $\Sigma^\pm \rightarrow n + \pi^\pm$  because the branching ratios of  $\Sigma^\pm \rightarrow n + \pi^\pm + \gamma$  to  $\Sigma^\pm \rightarrow n + \pi^\pm$  depend appreciably on this pion-wave assignment.<sup>5</sup> They<sup>4</sup> analyzed these radiative decays assuming the effective weak Hamiltonian for  $\Sigma^\pm \rightarrow n + \pi^\pm$ ,

$$H_W = i(\bar{n}\gamma_\mu[a + a'\gamma_5]\Sigma^\pm)(\partial\pi^\mp/\partial x_\mu) + \text{H.c.}, \quad (1)$$

\* Work supported by the National Science Foundation.

† NDEA Title IV Predoctoral Fellow.

‡ Present address: Physics Department, Hokkaido University, Sapporo, Japan.

<sup>1</sup> R. D. Tripp, M. B. Watson, and M. Ferro-Luzzi, Phys. Rev. Letters **9**, 66 (1962).<sup>2</sup> M. Gell-Mann and A. Rosenfeld, Ann. Rev. Nucl. Sci. **7**, 454 (1957).<sup>3</sup> A preliminary work by R. B. Willmann and T. H. Groves, Phys. Letters **14**, 350 (1965), reports some evidence for the  $P$ -wave assignment to  $\Sigma^+ \rightarrow n + \pi^+$ .<sup>4</sup> S. Barshay, U. Nauenberg, and J. Schultz, Phys. Rev. Letters **12**, 76 (1964).<sup>5</sup> A preliminary work has been reported recently by U. Nauenberg, M. Bazin, H. Blumenthal, L. Seidlitz, S. Marateck, and R. J. Plano, Bull. Am. Phys. Soc. **10**, 467 (1965). This work favors the  $S$ -wave assignment to  $\Sigma^- \rightarrow n + \pi^-$  and the  $P$ -wave assignment to  $\Sigma^+ \rightarrow n + \pi^+$  based upon the calculation in Ref. 4.

where  $a$  and  $a'$  are real constants, and the electromagnetic Hamiltonian which consists of the direct term from (1) and the usual term,

$$H_A = -ie[(\bar{p}\gamma_\mu p) + \dots]A_\mu - (e/2)[(\mu_p/2m_p)\bar{p}\sigma_{\mu\nu}p + \dots]F_{\mu\nu}, \quad (2)$$

in both of which the particle symbols stand for the respective field operators, the dots for the obvious terms, and  $\mu_p$  is the anomalous magnetic moment of the proton in units of the nuclear magneton. Therefore, their analysis consists of four phenomenological inner-bremsstrahlung diagrams in Fig. 1. The alternative choice is the effective weak interaction of nonderivative type,

$$H_W = i(\bar{n}[b + b'\gamma_5]\Sigma^\pm)\pi^\mp + \text{H.c.}, \quad (3)$$

where  $b$  and  $b'$  are real constants, and the usual electromagnetic Hamiltonian (2). Direct computation shows that the matrix elements for  $\Sigma^\pm \rightarrow n + \pi^\pm + \gamma$  depend upon the type of the effective weak Hamiltonian assumed, though the difference is small and vanishes in the absence of the anomalous magnetic moments in (2).

One may ask if there is any way to justify the above use of the effective weak Hamiltonian, (1) or (3), based upon a supposedly more realistic theory of the weak interaction and, therefore, to determine the reliability of the results of the previous calculation.<sup>4</sup>

The purpose of the present paper is to present an answer to this question on the assumption that the pole approximation of Feldman, Matthews, and Salam<sup>6</sup> is valid in  $\Sigma^\pm \rightarrow n + \pi^\pm$ . It is shown in Sec. II that the radiative decay-matrix elements in this pole approximation become essentially the same as those of the phenomenological inner-bremsstrahlung diagrams as long as the anomalous magnetic moments of the  $\Sigma$  and  $\Lambda$  hyperons are at most of the order of magnitude of the

<sup>6</sup> G. Feldman, P. T. Matthews, and A. Salam, Phys. Rev. **121**, 302 (1961). The exact meaning of this pole-approximation was pointed out by M. Sugawara, Phys. Rev. **135**, B252 (1964).

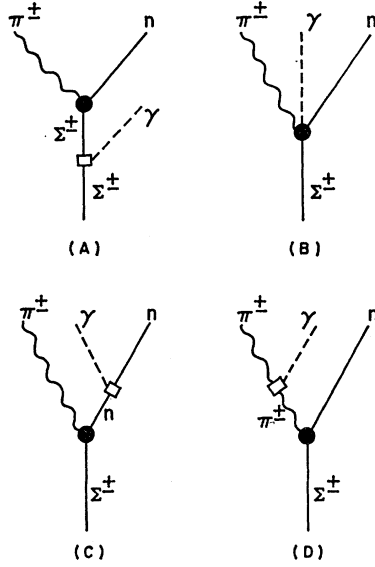


FIG. 1. The phenomenological inner-bremsstrahlung diagrams for  $\Sigma^\pm \rightarrow n + \pi^\pm + \gamma$  considered in Ref. 4. The solid circles stand for the effective weak vertices, and the open squares for the electromagnetic vertices. The branching ratios (7) and (8) do not include diagram B since the effective weak Hamiltonian of nonderivative type was assumed here.

nucleon magnetic moments. This is true independently of the signs and magnitudes of the strong and weak vertices involved. However, the numerical results which are summarized at the end of Sec. III differ from the results of the previous authors<sup>4</sup> mainly because their calculation considered only terms linear in the anomalous magnetic moments in the branching ratios. The conclusions of the present work are summarized at the end of Sec. III.

## II. RADIATIVE PIONIC DECAYS IN THE POLE APPROXIMATION

In the pole approximation,<sup>6</sup> the decays  $\Sigma^\pm \rightarrow n + \pi^\pm$  are described in terms of the pole diagrams shown in Fig. 2. The matrix elements for these decays can be obtained by the lowest order covariant calculation when the strong and weak vertices in Fig. 2 are described by the effective Hamiltonians,

$$H_S = ig(\bar{N}\gamma_5\tau N) \cdot \pi + \dots \quad (4)$$

in terms of the usual isospin formalism, and

$$H_W = (\bar{n}[c + c'\gamma_5]\Lambda) + \dots \quad (5)$$

in terms of real constants  $c$  and  $c'$ , where the dots stand for the obvious terms.

If the electromagnetic Hamiltonian (2) is included in addition to (4) and (5), the lowest order covariant calculation yields the decay-matrix elements for the radiative decays  $\Sigma^\pm \rightarrow n + \pi^\pm + \gamma$ . These decay-matrix elements consist of the twelve diagrams, shown in Fig. 3, for each of  $\Sigma^\pm \rightarrow n + \pi^\pm + \gamma$ .<sup>7</sup>

<sup>7</sup> We do not include in Fig. 3 those diagrams with the transition-moment or those diagrams which include virtual  $\Sigma^0 \leftrightarrow \Lambda^0$  electromagnetic transitions. These diagrams do not appreciably affect our results as long as the transition moment is at most of the order of magnitude of the nucleon magnetic moments.

It can be shown that there is a simple correspondence between the phenomenological inner-bremsstrahlung diagrams in Fig. 1 and the pole diagrams in Fig. 3.<sup>7</sup> For example the sum of diagrams (a), (b), (e), and (i) of Fig. 3 correspond to the diagram (A) of Fig. 1. This correspondence is exact in the absence of the Pauli terms in (2), and also is completely independent of the various coupling constants in (4) and (5). The correspondence is due to an identity relation satisfied by the energy denominators resulting from the pole diagrams. For example, in the case of (a) and (b) of Fig. 3, this identity relation reads

$$\begin{aligned} & [(p-k)^2 + m_p^2]^{-1} [(p-k)^2 + m_\Sigma^2]^{-1} \\ & + [(p-k)^2 + m_p^2]^{-1} [p^2 + m_p^2]^{-1} \\ & = [(p-k)^2 + m_\Sigma^2]^{-1} [p^2 + m_p^2]^{-1}, \quad (6) \end{aligned}$$

where  $p$  and  $k$  are the four-momenta of  $\Sigma^+$  and the photon, respectively. In the presence of the Pauli terms in (2), the correspondence is only approximate. However, one can verify by direct computation that all those extra terms which destroy the exact correspondence are negligible as long as the anomalous magnetic moments of the  $\Sigma$  and  $\Lambda$  hyperons are at most of the order of magnitude of the nucleon magnetic moments. Similarly, the sum of diagrams (c), (f), (g), (j), and (k) in Fig. 3 corresponds to diagram (C) in Fig. 1, while the sum of (d), (h), and (l) in Fig. 3 is always in exact correspondence to diagram (D) in Fig. 1 since there are no Pauli terms for the pion. Thus the pole diagrams with (2), (4), and (5) assumed differ only slightly from the phenomenological inner-bremsstrahlung diagrams when the effective Hamiltonians (2) and (4) are assumed, though the expressions become much more complicated for the pole diagrams.

## III. RESULTS AND CONCLUSIONS

Because of the correspondence discussed in the previous section between the pole diagrams and the phenomenological inner-bremsstrahlung diagrams, the results below refer to the inner-bremsstrahlung matrix

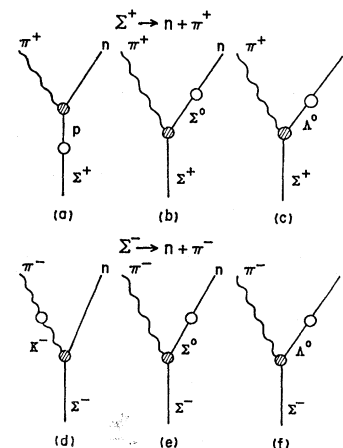


FIG. 2. The pole diagrams for  $\Sigma^\pm \rightarrow n + \pi^\pm$ . The shaded circles stand for the strong vertices, and the open ones for the weak vertices.

elements summarized in Fig. 1. The effective weak Hamiltonian of the nonderivative type (3) and the usual electromagnetic Hamiltonian (2) are assumed. The following results are in qualitative agreement with the results when the effective weak Hamiltonian (1) and the electromagnetic Hamiltonian (2) together with the direct term from (1) are used.

The branching ratios of  $\Sigma^\pm \rightarrow n + \pi^\pm + \gamma$  to  $\Sigma^\pm \rightarrow n + \pi^\pm$  are given as functions of the pion momentum  $q$  in the  $\Sigma$  rest system by

$$\begin{aligned} \left(\frac{dB^\pm}{dq}\right)_S &= (e^2/4\pi)(q/\pi Qq_0) \left\{ \left(\frac{Q_0 - q_0}{2(m_\Sigma + m_N - Q_0)}\right) F_1(q) \right. \\ &+ \left(\frac{q}{(Q_0 - q_0)}\right) [F_2(q) - 2q/q_0] + \left(\frac{m_\Sigma}{m_\Sigma + m_N - Q_0}\right) \\ &\times \left[ [(\mu_{\Sigma^\pm})^2 + (\mu_n)^2] \left(\frac{(m_\Sigma + m_N - q_0)}{4m_N^2}\right) F_3(q) - \frac{F_4(q)}{8m_N^2} \right] \\ &- (\mu_{\Sigma^\pm})(\mu_n) \left(\frac{\alpha}{4m_N^2} F_1(q) + \frac{F_3(q)}{2m_N} + \frac{F_4(q)}{8\alpha}\right) \\ &\left. \pm [(\mu_{\Sigma^\pm}) - (\mu_n)] \left(\frac{\alpha}{2m_\Sigma m_N} F_1(q) + \frac{F_3(q)}{2m_\Sigma}\right) \right\}, \quad (7) \end{aligned}$$

where the top and bottom signs in (7) refer to  $\Sigma^+ \rightarrow n + \pi^+ + \gamma$  and  $\Sigma^- \rightarrow n + \pi^- + \gamma$ , respectively, and the pion in  $\Sigma^\pm \rightarrow n + \pi^\pm$  is in the  $S$ -wave state; and

$$\begin{aligned} \left(\frac{dB^\pm}{dq}\right)_P &= (e^2/4\pi)(q/\pi Qq_0) \left\{ \left(\frac{Q_0 - q_0}{2(m_\Sigma - m_N - Q_0)}\right) F_1(q) \right. \\ &+ \left(\frac{q}{(Q_0 - q_0)}\right) [F_2(q) - 2q/q_0] + \left(\frac{m_\Sigma}{m_\Sigma - m_N - Q_0}\right) \\ &\times \left[ [(\mu_{\Sigma^\pm})^2 + (\mu_n)^2] \left(\frac{(m_\Sigma - m_N - q_0)}{4m_N^2}\right) F_3(q) - \frac{F_4(q)}{8m_N^2} \right] \\ &+ (\mu_{\Sigma^\pm})(\mu_n) \left(\frac{\alpha}{4m_N^2} F_1(q) - \frac{F_3(q)}{2m_N} + \frac{F_4(q)}{8\alpha}\right) \\ &\left. \pm [(\mu_{\Sigma^\pm}) + (\mu_n)] \left(\frac{\alpha}{2m_\Sigma m_N} F_1(q) - \frac{F_3(q)}{2m_\Sigma}\right) \right\}, \quad (8) \end{aligned}$$

where the top and bottom signs in (8) refer to  $\Sigma^+ \rightarrow n + \pi^+ + \gamma$  and  $\Sigma^- \rightarrow n + \pi^- + \gamma$ , respectively, and the pion in  $\Sigma^\pm \rightarrow n + \pi^\pm$  is in the  $P$ -wave state. In (7) and (8),  $(\mathbf{Q}, iQ_0)$  and  $(\mathbf{q}, iq_0)$  are the pion four-momenta in  $\Sigma^\pm \rightarrow n + \pi^\pm$  and  $\Sigma^\pm \rightarrow n + \pi^\pm + \gamma$ , respectively, and

$$\begin{aligned} \alpha &= m_\Sigma(Q_0 - q_0), \\ F_1(q) &= \ln[(m_\Sigma - q_0 + q)/(m_\Sigma - q_0 - q)], \\ F_2(q) &= \ln[(q_0 + q)/(q_0 - q)], \\ F_3(q) &= 2\alpha q / (m_\Sigma^2 + m_\pi^2 - 2m_\Sigma q_0), \\ F_4(q) &= 4\alpha^2 q (m_\Sigma - q_0) / (m_\Sigma^2 + m_\pi^2 - 2m_\Sigma q_0)^2. \end{aligned} \quad (9)$$

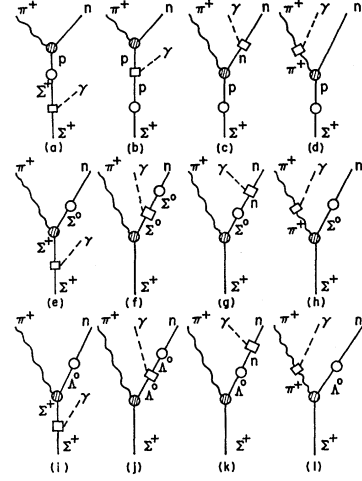


FIG. 3. The diagrams for  $\Sigma^+ \rightarrow n + \pi^+ + \gamma$  in the pole approximation. The shaded circles stand for the strong vertices, the open circles for the weak vertices, and the open squares for the electromagnetic ones. The diagrams for  $\Sigma^- \rightarrow n + \pi^- + \gamma$  can be obtained from Fig. 2 similarly.

Also, the masses of the particles in (7), (8), and (9) have been replaced by the average masses of the respective isospin multiplets for computational convenience. The anomalous magnetic moments of  $\Sigma^\pm$  ( $\mu_{\Sigma^+}$  and  $\mu_{\Sigma^-}$ ) and the anomalous magnetic moment of the neutron ( $\mu_n$ ) in (7) and (8) are all in units of the nuclear magneton.

The branching ratios which are given in (7) and (8) as functions of pion momentum in the  $\Sigma$  rest system show significant differences which can be used to determine the orbital angular momentum of the pion in  $\Sigma^\pm \rightarrow n + \pi^\pm$ . The most important pion-momentum range for this purpose is  $80 \text{ MeV}/c \leq q \leq 140 \text{ MeV}/c$ ,

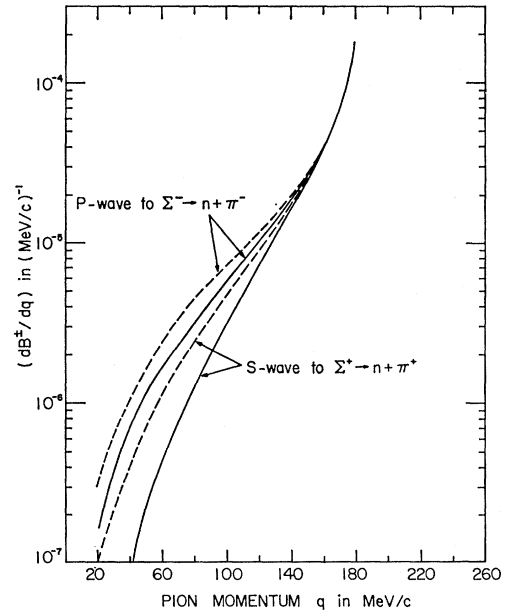


FIG. 4. The branching ratios (7) and (8) versus the pion momentum in the rest system of  $\Sigma$ . The solid curves correspond to (i) when all the anomalous magnetic moments are neglected. The dashed curves correspond to (ii) when  $\mu_{\Sigma^+} = 3.5$  and  $\mu_{\Sigma^-} = -3.5$  in units of the nuclear magneton, and  $\mu_n$  has its measured value.

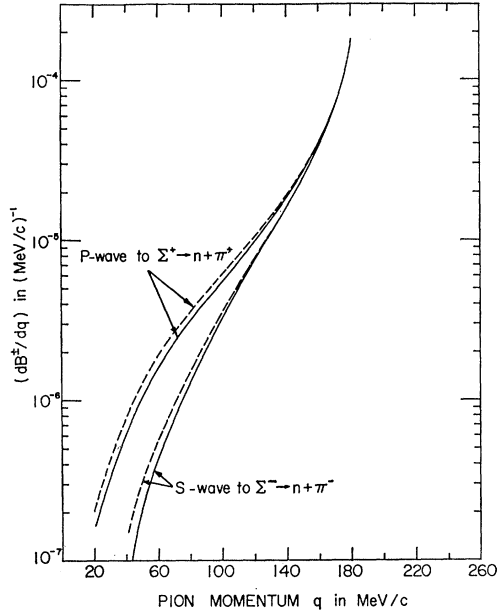


FIG. 5. The branching ratios (7) and (8) versus the pion momentum in the rest system of  $\Sigma$ . The solid curves correspond to (i) when all the anomalous magnetic moments are neglected. The dashed curves correspond to (ii) when  $\mu_{\Sigma^+}=3.5$  and  $\mu_{\Sigma^-}=-3.5$  in the units of the nuclear magneton, and  $\mu_n$  has its measured value.

since below this range the branching ratios are too small to be measured while above this range the branching ratios are essentially identical. Examination of (7) and (8) for the above momentum range shows that the terms due to the anomalous magnetic moments are not negligible compared with the terms due to the electric charge. Figures 4 and 5 compare these branching ratios when (i) all the anomalous magnetic moments are neglected, and when (ii)  $\mu_{\Sigma^+}=+3.5$ <sup>8</sup> and  $\mu_{\Sigma^-}=-3.5$

TABLE I. The integrated branching ratios ( $\times 10^{-4}$ ) for  $\Sigma^- \rightarrow n + \pi^-$  taken from Figs. 4 and 5, for the pion-momentum range and the anomalous magnetic moments  $\mu_{\Sigma^-}$  and  $\mu_n$  indicated.

Anomalous magnetic moments in units of the nuclear magneton	Pion-momentum range		
	$0 \leq q \leq 120$ MeV/c	$0 \leq q \leq 140$ MeV/c	$0 \leq q \leq 160$ MeV/c
(A) When <i>S</i> wave is assigned to $\Sigma^- \rightarrow n + \pi^-$ :			
$\mu_{\Sigma^-}=0, \mu_n=0$	1.8	4.1	9.8
$\mu_{\Sigma^-}=-3.5, \mu_n=-1.91$	1.9	4.3	10
(B) When <i>P</i> wave is assigned to $\Sigma^- \rightarrow n + \pi^-$ :			
$\mu_{\Sigma^-}=0, \mu_n=0$	3.3	6.1	12
$\mu_{\Sigma^-}=-3.5, \mu_n=-1.91$	4.2	7.4	14

<sup>8</sup> A. D. McInturf and C. E. Roos, Phys. Rev. Letters 13, 246 (1964), report that the total magnetic moment of  $\Sigma^+$  is approximately 4.3 nuclear magnetons.

TABLE II. The integrated branching ratios ( $\times 10^{-4}$ ) for  $\Sigma^+ \rightarrow n + \pi^+$  taken from Figs. 4 and 5, for the pion-momentum range and the anomalous magnetic moments  $\mu_{\Sigma^+}$  and  $\mu_n$  indicated.

Anomalous magnetic moments in units of the nuclear magneton	Pion-momentum range		
	$0 \leq q \leq 120$ MeV/c	$0 \leq q \leq 140$ MeV/c	$0 \leq q \leq 160$ MeV/c
(A) When <i>S</i> wave is assigned to $\Sigma^+ \rightarrow n + \pi^+$ :			
$\mu_{\Sigma^+}=0, \mu_n=0$	1.8	4.1	9.8
$\mu_{\Sigma^+}=+3.5, \mu_n=-1.91$	2.6	5.3	11
(B) When <i>P</i> wave is assigned to $\Sigma^+ \rightarrow n + \pi^+$ :			
$\mu_{\Sigma^+}=0, \mu_n=0$	3.3	6.1	12
$\mu_{\Sigma^+}=+3.5, \mu_n=-1.91$	3.5	6.5	13

in units of the nuclear magneton, and  $\mu_n$  has its measured value. The integrated branching ratios for the cases (i) and (ii) above are given in Tables I and II. These figures and tables illustrate that the anomalous magnetic moments can have a noticeable effect on the branching ratios, (7) and (8). However, for the particular values of  $\mu_{\Sigma^\pm}$  which are used in (ii), there occur cancellations among the terms due to the anomalous magnetic moments when the pions in  $\Sigma^+ \rightarrow n + \pi^+$  and  $\Sigma^- \rightarrow n + \pi^-$  are in the *P*-wave and *S*-wave states, respectively.

The effect on the branching ratios due to a small admixture of the opposite wave was estimated. It is found that, as long as the constants  $c$  and  $c'$  in the effective weak Hamiltonian (5) are real, this effect amounts to a change of approximately 1% in the branching ratios even when the asymmetry parameters are the largest consistent with experiments.<sup>1</sup>

The conclusions of the present work can be summarized as follows:

(1) If the pole approximation<sup>6</sup> is valid, the radiative decays  $\Sigma^\pm \rightarrow n + \pi^\pm + \gamma$  are well described by the inner-bremsstrahlung diagrams provided the anomalous magnetic moments of the  $\Sigma$  and  $\Lambda$  hyperons are at most of the order of magnitude of the nucleon magnetic moments. Since the branching ratios of  $\Sigma^\pm \rightarrow n + \pi^\pm + \gamma$  to  $\Sigma^\pm \rightarrow n + \pi^\pm$  depend on the pion-wave assignment in  $\Sigma^\pm \rightarrow n + \pi^\pm$ , these radiative decay modes can be used to determine the angular momenta of the pions in  $\Sigma^\pm \rightarrow n + \pi^\pm$ . This is in general agreement with the previous authors.<sup>4</sup>

(2) However, the present analysis shows that the anomalous magnetic moments can noticeably affect the branching ratios of  $\Sigma^\pm \rightarrow n + \pi^\pm + \gamma$  to  $\Sigma^\pm \rightarrow n + \pi^\pm$ , in contrast with the previous authors.<sup>4</sup> Thus, in order to check the underlying theoretical assumptions so as to determine the pion-wave assignment in  $\Sigma^\pm \rightarrow n + \pi^\pm$ , it is necessary to have either very accurate data for  $\Sigma^\pm \rightarrow n + \pi^\pm + \gamma$  or an experimental determination of the anomalous magnetic moments of  $\Sigma^\pm$ .<sup>8</sup>